Applied Surface Science 258 (2012) 3289–3297

Contents lists available at SciVerse ScienceDirect

Applied Surface Science

journal homepage: www.elsevier.com/locate/apsusc

Physico-chemical properties of Pd nanoparticles produced by Pulsed Laser Ablation in different organic solvents

Gabriele Cristoforetti[a,*], Emanuela Pitzalis[b], Roberto Spiniello[b], Randa Ishak[c], Francesco Giammanco[d], Maurizio Muniz-Miranda[e], Stefano Caporali[e]

[a] National Institute of Optics, Research Area of National Research Council, Via G. Moruzzi 1, 56124 Pisa, Italy
[b] Institute of Chemistry of OrganoMetallic Compounds, Research Area of National Research Council, Via G. Moruzzi 1, 56124 Pisa, Italy
[c] Department of Chem. Eng. And Material Science, University of Pisa, Via Diotisalvi 2, 56126 Pisa, Italy
[d] Department of Physics, University of Pisa, Largo B. Pontecorvo 3, 56127 Pisa, Italy
[e] Department of Chemistry, University of Florence, Via della Lastruccia 3, 50019 Sesto Fiorentino, Italy

ARTICLE INFO

Article history:
Received 21 July 2011
Received in revised form 8 November 2011
Accepted 17 November 2011
Available online 26 November 2011

Keywords:
Pulsed Laser Ablation in Liquid
Palladium nanoparticles
Organic solvents
Nanoparticles synthesis

ABSTRACT

Palladium nanoparticles are arousing an increasing interest because of their strong activity in heterogeneous catalysis in a wide range of reactions. Driven by the interest of producing Pd nanoparticles to be deposited for catalysis over hydrophobic supports, we investigated their synthesis via Pulsed Laser Ablation in Liquid in several organic solvents, as acetone, ethanol, 2-propanol, toluene, n-hexane. The colloids were produced by using a Nd:YAG ns laser and without the addition of surfactant agents. The morphology, composition, stability and oxidation state of the obtained nanoparticles were investigated by TEM-EDS analysis, UV–vis spectroscopy, X-ray Photoelectron Spectroscopy and micro-Raman spectroscopy. The results evidence that the nature of the solvent influences both the yield and the physico-chemical properties of the produced nanoparticles. While in acetone and alcohols spheroidal, non aggregated and stable particles are obtained, in case of toluene and n-hexane few unstable particles surrounded by a gel-like material are produced. Raman/XPS measurements suggest the presence of amorphous or graphitic carbon onto crystalline Pd nanoparticles, which could have hindered their growth and determined the observed smaller sizes if compared to nanoparticles produced in water. The stability of Pd colloids obtained in acetone and alcohols was attributed to adsorbed anions like enolates or alcoholates; non polar solvents like toluene and n-hexane, unable to give rise to adsorbed anionic species, cannot provide any stabilization to the palladium nanoparticles. XPS analyses also evidenced a partial oxidation of particles surface, with a ratio Pd^{2+}:Pd^{0} of 1:2.5 and 1:4 in acetone and ethanol, respectively.

1. Introduction

In the framework of the current research on the development of nanoparticles/nanostructures production techniques, Pulsed Laser Ablation in Liquid (PLAL) recently attracted a large interest in the scientific community, resulting in a considerable effort both focussed in improving the knowledge of the physical and chemical processes involved and in testing its effectiveness for a widespread range of applications.

The growing interest in PLAL [1] relies in its capability of producing stable and pure nanoparticles (NPs), devoid of chemical contaminants such as surfactants or precursor agents. The bare surface of NPs is particularly attractive for applications exploiting their surface chemical properties, such as those involving their functionalization with (bio-) molecules [2,3] or those utilizing their catalytic effect. This motivated some research groups to investigate the possibility of synthesizing Ni, Pt and Pd nanoparticles [4–9], which seem very promising for catalytic purposes, testing the influence of experimental parameters on NP morphology and their catalytic effectiveness in specific reactions. Among these elements, palladium is very appealing because is active in heterogeneous catalysis in a wide range of reactions, including hydrogenations, oxidations, hydrodechlorinations and C–H bond activation. In particular, Pd supported nanoparticles have been used in reactions involving C–C bond formation, e.g. Suzuki, Heck, Sonogashira and related C–C coupling reactions [10]. For this reason, the preparation of Pd nanoparticles with several techniques and the properties of particles deposited on different supports, along with their behavior in catalysis, have been thoroughly investigated [11].

In a previous work [12] we studied the production of Pd nanoparticles in pure water, with and without the addition of sodium dodecyl sulfate as surfactant, investigating the influence

* Corresponding author. Tel.: +39 0503152222; fax: +39 0503152576.
E-mail address: gabriele.cristoforetti@cnr.it (G. Cristoforetti).

0169-4332/$ – see front matter © 2011 Elsevier B.V. All rights reserved.
doi:10.1016/j.apsusc.2011.11.084

of laser pulse energy and beam focussing conditions on NP morphology and stability. The aim of the present work is extending the research to the synthesis of Pd NPs in organic solvents, like ethanol, 2-propanol, acetone, toluene and n-hexane, focussing the attention on the relation between the solvent nature, the laser fluence and the properties of the NPs formed (morphology, stability, surface chemistry). The interest in obtaining Pd colloids in organic solvents is mainly dictated by their usefulness in the preparation of Pd nanoparticles supported on hydrophobic supports [13].

It is well known that the synthesis is dependent on the nature of the solvent used, since a different composition, structure or polarity of its molecules results in a different interaction with the NPs, thus strongly affecting their growth, final composition and stability. It was shown, in fact, that species resulting from the solvent can attach to or react with NPs, changing their composition or resulting in an external coating. Furthermore, solvent molecules in the solution can bind or adsorb to NPs surface hindering their growth and aggregation, making the colloid stable with time. The importance of the nature of the solvent in determining the composition, size/morphology and stability of the nanoparticles, is verified in numerous papers [14–19].

For these reasons, in the present work, beyond a morphological characterization of Pd NPs produced in the different solvents, we investigated the composition and the oxidation state of the particles, and tried to relate these data with the stability of the nanoparticles.

This work, beyond testing the capability of PLAL in synthesizing Pd NPs in organic solvents, is aimed at improving the knowledge of the role of solvent during the process of nanoparticle growth and subsequent stabilization. In fact, in spite of the large amount of experimental works on this topic, it is not yet available a quantitative model able to describe but mostly to predict the growth and stabilization of nanoparticles given the production parameters, such as laser energy and fluence, and the ambient solvent.

2. Experimental

The experimental setup used for the production of Pd nanoparticles is the same described in Ref. [12], and will be briefly summarized in the following.

A Nd:YAG laser pulse (τ = 12 ns), operating at a repetition rate of 10 Hz and at the fundamental wavelength (λ = 1064 nm), was focussed onto the target surface at normal incidence by means of a lens of 25 cm focal length. Relying on the optimization of laser focussing conditions reported previously [12], the Lens-To-Sample-Distance was fixed at 19 cm, resulting in a quite large irradiated spot (diameter $\approx$ 500 μm) and then in a larger amount of material ablated. Nanoparticles were produced by using a laser pulse energy of 7 and 38 mJ, corresponding to fluences of $\sim$4 and 21 J cm^{-2} (irradiances of 0.33 and 1.75 GW cm^{-2}). The target was a pure palladium plate with purity > 99.9%, fixed at the bottom of a glass vessel filled with 8 ml (height above the target = 4 mm) of liquid. Each stage of NP production lasted for 20 min, during which time the glass vessel was rotated and translated in order to prevent effects due to crater formation.

Different organic solvents, i.e. acetone, toluene, n-hexane, ethanol and 2-propanol, were used during the ablation and the NPs obtained were compared with those formed in ultrapure (u.p.) water. No surfactant agents were used for the stabilization of the colloid. During the ablation process a non negligible fraction of volatile solvents evaporated, which was particularly severe for acetone and/or when the largest pulse energy (E = 38 mJ) were used. In case of solvent evaporation, the glass vessel was refilled-up during the process maintaining it at the initial level.

The produced colloids were analyzed by UV–vis spectroscopy on a PerkinElmer Lambda 25 UV–vis spectrometer, using quartz cells (Hellma) with 10 mm light path. UV–vis spectra were measured 24 h and, successively, 30 days after the production stage to evaluate the stability of the nanoparticles over time.

Particle morphology and size distribution were investigated using TEM-EDS analysis performed on Philips CM12 microscope working at 120 kV equipped with Bruker Quantax EDX analysis. Few drops of the supernatant colloid solution were placed on a carbon coated copper grid and allowed to dry at a temperature around 80 °C. The deposition of colloidal drops on the copper grid was performed a couple of days after the production stage, when the most part of the aggregated unstable material in the solution had been already collapsed on the bottom of the vial where NPs were contained.

TEM images were analyzed using a semi-automatic plug-in of the ImageJ software to determine the NPs size distribution. A quantity of at least 300 nanoparticles was measured for each sample.

The crystalline structure of the NPs has been verified using the Selected Area Electron Diffraction (SAED) technique in TEM and in HR-TEM.

The oxidation state of Pd nanoparticles was investigated by X-ray Photoelectron Spectroscopy (XPS) using a non-monochromated Mg-Kα X-ray source (1253.6 eV) and a VSW HAC 5000 hemispherical electron energy analyzer operating in the constant-pass-energy mode at E_{pas} = 44 eV. The samples were prepared just before the analysis depositing few drops of the colloidal solution on a soda glass substrate and letting the solvent to evaporate. In order to increase the amount of NPs deposited on the surface, this procedure was repeated several times. Then, the NP-loaded glass was introduced in the UHV system via a loadlock under inert gas (N_2) flux, and it was kept in the introduction chamber for at least 12 h, allowing the removal of volatile substances such as water and organic solvents, as confirmed by the pressure value achieved (2×10^{-9} mbar), just above the instrument base pressure. The obtained spectra were referenced to C 1s peak at 284.8 eV assigned to the adventitious carbon and the recorded peaks were fitted using XPSPeak 4.1 software employing Gauss–Lorentz curves after subtraction of a Shirley-type background.

A micro-Raman characterization (Renishaw RM2000) of the nanoparticles produced and of the material deposited at the bottom of the vial, after a proper deposition onto a steel substrate, was performed, by using an Ar+ laser source emitting at 514.5 nm. Sample irradiation was accomplished using the $\times$100 microscope objective of a Leica Microscope DMLM. The beam power was $\sim$3 mW, the laser spot diameter was adjusted between 1 and 3 μm. Raman scattering was filtered by a double holographic Notch filters system and collected by an air cooled CCD detector. The acquisition time for each measurement was 10 s. All spectra were calibrated with respect to a silicon wafer at 520 cm^{-1}.

3. Results

After a few minutes of laser irradiation, all the solutions, except in the case of n-hexane, changed to yellow and successively to brown, when the NP concentration became higher. Differently, laser irradiation into n-hexane resulted in a slightly opalescent solution, without any appreciable change of colour. In all the cases, when the lowest pulse energy was used, the formation of a plasma plume at the target surface was clearly visible. Conversely, when operating at the largest irradiance, at first a plasma formed at the target surface but successively – after a few tens of seconds – a secondary plasma became visible at the air–solvent interface, which was associated to a strong reduction of the brightness the primary plasma. Such phenomenon, whose threshold in ultrapure

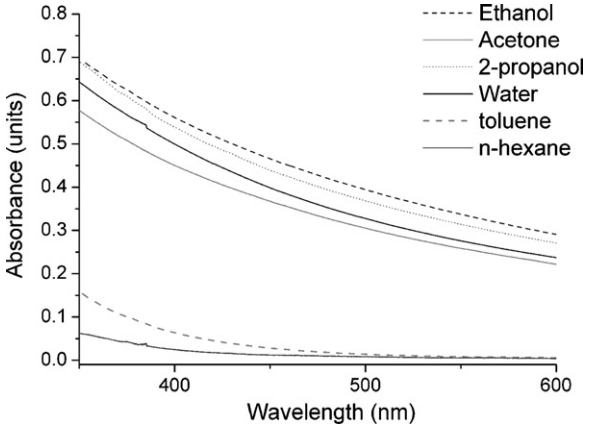

Fig. 1. Extinction spectra of Pd colloids prepared in different solvents by using a fluence of 21 J cm^{-2}. The contribution due to the pure solvent has been subtracted from the spectra.

water was measured in a previous work [12] at ~12 J cm^{-2} (e.g. two orders of magnitude lower that the breakdown threshold of pure water), is probably associated to the progressive increase of nanoparticles density in the solution. Due to the interaction with the laser beam such particles emit electrons by thermoionic effect or, more unlikely, by multiphoton ionization (Work Function of bulk palladium ≈5.12 eV ≈ 4.4$h\nu$) [20,21], which can in turn ignite laser absorption and generate the secondary plasma via inverse Bremsstrahlung processes. The absorption of part of the laser energy by the secondary plasma at air–solvent interface produces a consequent reduction of mass removal from the target. Thus, this effect makes the ablation process time-dependent (e.g. larger during the early laser shots and lower during the successive ones). Another drawback of secondary plasma is the possible ignition of solvent combustion during the experiment. In our case, combustion of all the solvents except toluene occurred when laser energy was increased beyond 50 mJ.

UV–vis extinction spectra of the colloids exhibit a significant absorption rising in the UV, typical of an interband transition of a metallic system, which is in qualitative agreement with the Mie theory [22] and with experimental UV–vis curves of Pd NPs reported in literature [23,24]. No peak due to plasmon resonance is evident in the spectra. In the case of acetone, the spectrum is useless at wavelengths lower than 330 nm, where the light probe is completely absorbed by the solvent. The extinction spectra of the different colloids are reported in Fig. 1, together with the spectra of Pd colloid obtained in ultrapure water.

According to the Mie theory in the quasi-static approximation (valid for particles much smaller than the probing wavelength), the main contribution of the absorbance is dipolar absorption, which is proportional to the total volume of the particles [25]. Therefore, a qualitative comparison of the total mass of nanoparticles in the different colloids, still dispersed in the solution, can be obtained using the expression of dipolar absorption at a fixed wavelength within the interband absorption band (in our case we consider λ = 340 nm) and with the proper value of the dielectric constant of the solvent. According to the above estimation of mass of the NPs we obtain $M_{\text{ethanol}} \approx M_{\text{2-propanol}} > \sim M_{\text{water}} > \sim M_{\text{acetone}} > M_{\text{toluene}} > M_{\text{n-hexane}}$, where the mass calculated in the last two cases is significantly lower than in the other cases. Nevertheless, this approach cannot provide an accurate estimation of NPs mass because it relies on the purity of Pd particles, while actually they include a non negligible component of carbon and oxygen atoms, as will be shown in the following. The above results can be compared with the ablation rates calculated by AAS for the different solvents, which account for the total weight of mass removed from the target, thus including

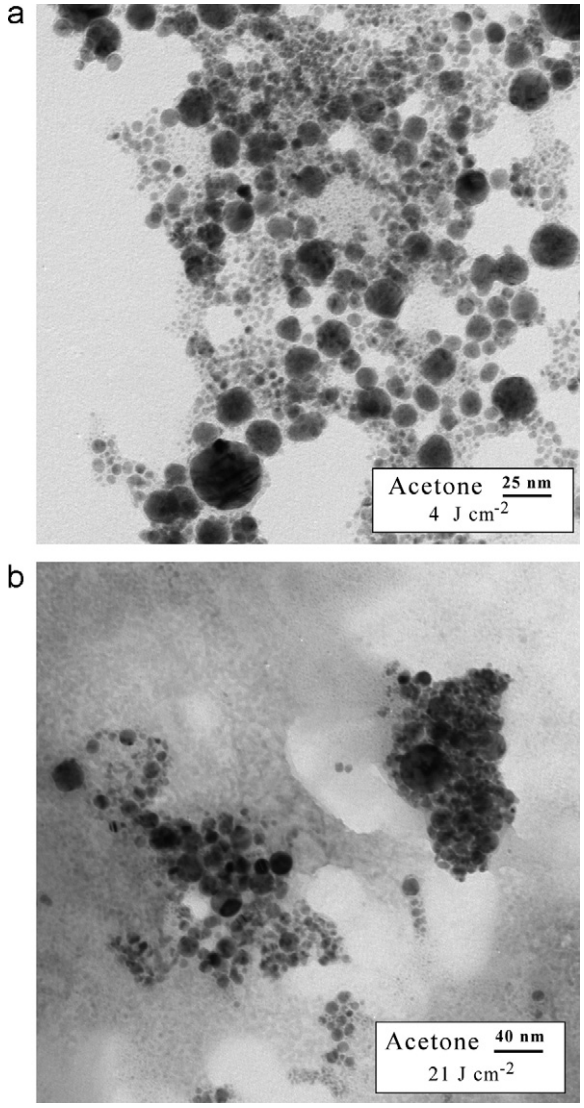

Fig. 2. TEM images of colloids produced in acetone at different laser fluences.

also the material already collapsed and deposited on the bottom. The larger ablation rate is obtained for ethanol, 2-propanol and acetone (mass removed ~0.16 mg), followed by water (~0.13 mg), toluene (~0.025 mg) and n-hexane (<0.01 mg). These values qualitatively agree with the trend of NPs mass obtained via UV–vis spectroscopy, where minor discrepancies (i.e. acetone) will be discussed later, and show that the efficiency of laser ablation in different solvents can largely differ not only for the different degree of beam absorption by the solvent (which is in our case not relevant except for water) but also for the dielectric constants (affecting laser beam focussing), and other features as density and thermodynamic properties (affecting breakdown of the solvent and plasma plume formation).

3.1. Acetone

The UV–vis spectra of the colloids in acetone acquired 1 day and 1 month after their production are substantially identical, suggesting a strong stability of the nanoparticles with no evidence of precipitate even after 1 month.

TEM images of NPs ensembles obtained in acetone at 4 and 21 J cm^{-2} laser fluences are reported in Fig. 2. In case of larger fluence, nanoparticles ensembles are surrounded by a dark gel-like

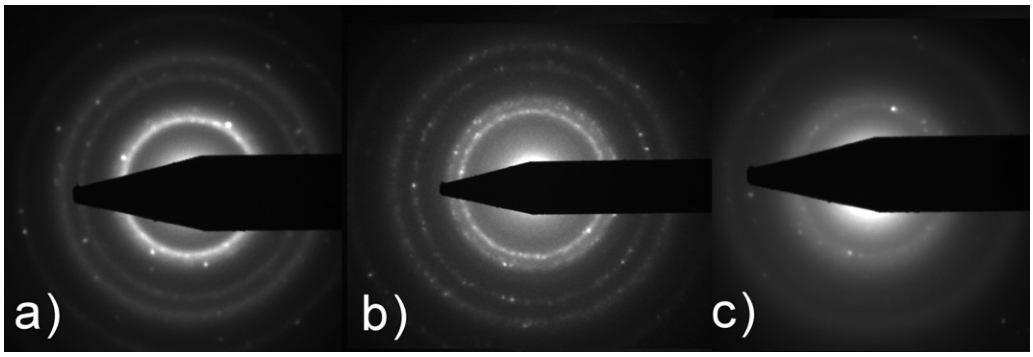

Fig. 3. SAED patterns of nanoparticles subsets in acetone (a) and in ethanol (b) and of gel-like material in toluene (c).

material. SAED pattern obtained from a subset of NPs at 21 J cm^{-2} suggests a large part of crystalline material accompanied by some amorphous stuff (see Fig. 3a).

At low fluence, NPs are spheroidal and non aggregated, which makes this condition more attractive for NP production. The distribution of their sizes, as visible in Fig. 4, is quite narrow (σ = 2 nm), with an average size of 3.3 nm. However, the amount of small sized particles (<3 nm) is probably underestimated, so that the average size can even lower. The size distribution at low fluence can be satisfactorily fitted by a lognormal function, with a slight excess of large particles (see the inset in Fig. 4).

XPS analysis of the colloid obtained at low fluence was performed in order to gather information on the elementary composition of the nanoparticles and the prevailing oxidation state of the elements. The peaks $3d_{5/2}$ e $3d_{3/2}$ of Pd have an evident asymmetric shape, suggesting a combination of different oxidation states (Fig. 5). The best fitting of the experimental data is achievable by means of two doublets. In accordance with the Binding Energy values reported in literature [26–28], the two contributions can be reasonably assigned to metallic palladium (Pd^0, $3d_{5/2}$ at 335.2 ± 0.1 eV) and palladium in the +2 oxidation state ($3d_{5/2}$ at 337.1 ± 0.1 eV). The ratio of the palladium atoms in these two states for the portion of sample probed by XPS (in these conditions about 3–4 nm), was determined by the ratio of their relative peak areas as being approximately 1:2.5 (Pd^{2+}:Pd^0).

Beyond the peaks relative to Pd and to other elements attributable to the glass substrate (O, Si, Na), a strong signal deriving from carbon is visible (see Fig. 5). The good signal-to-noise ratio allowed a significant fitting of the peak by means of 3 contributions, where the strong one is centred at a Binding Energy value of 284.8 eV, compatible with the aliphatic carbon and/or C^0. The other contributions, located at higher energy values (~286 and 288 eV), can be attributable to oxidized states of carbon, respectively to carbon in alcohols/ethers and carboxyl groups. In order to identify the origin of carbon in XPS analysis, the same measurement was

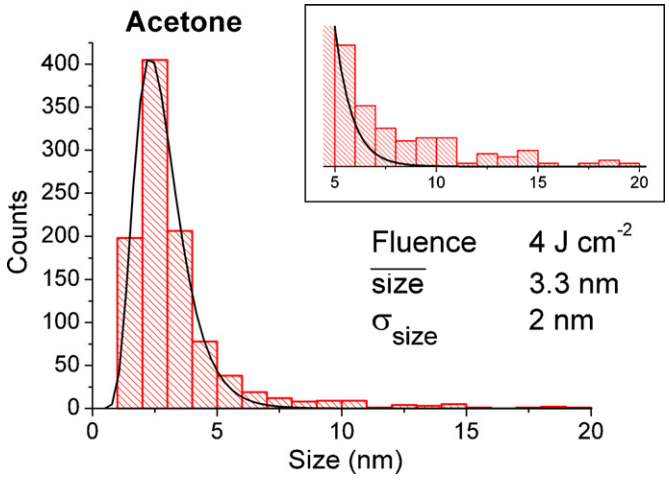

Fig. 4. Size distribution of nanoparticles produced in acetone with 4 J cm^{-2} laser fluence. The solid line represents the fit of the data by using a single log-normal function. In the inset a magnification of the region of larger size NPs is reported, showing the excess of particles with respect to the lognormal curve fitting.

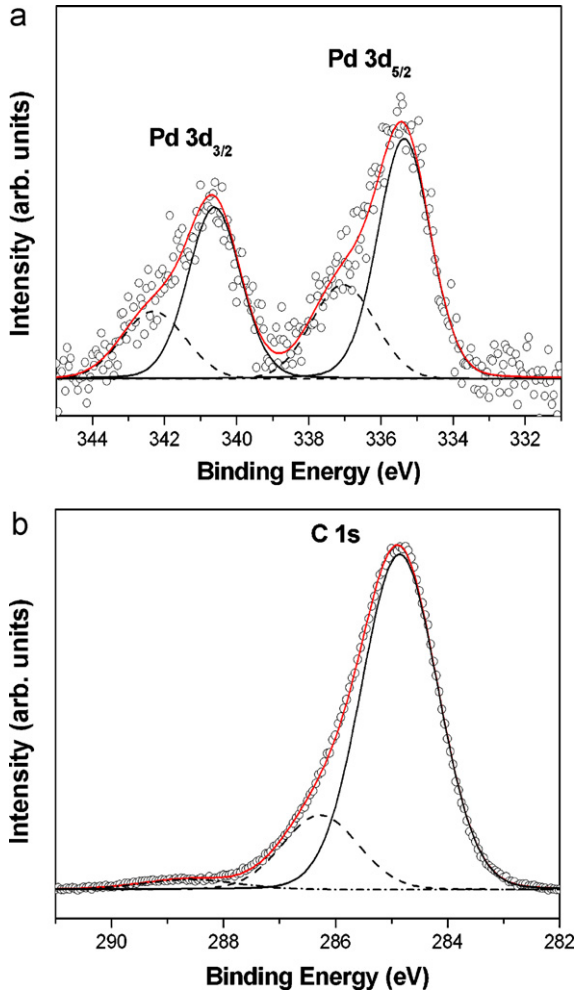

Fig. 5. XPS spectrum (circles represent row data) of NPs in acetone. On the left is displayed the region of spectrum characteristic of the Pd 3d transitions; the solid curve refers to Pd^0 whereas the dashed curve refers to Pd^{2+}. On the right the region of spectrum characteristic of C 1s transition is displayed. The solid, dash and dash-dot curves refer to aliphatic, alcohols/ethers and carboxyls carbon respectively.

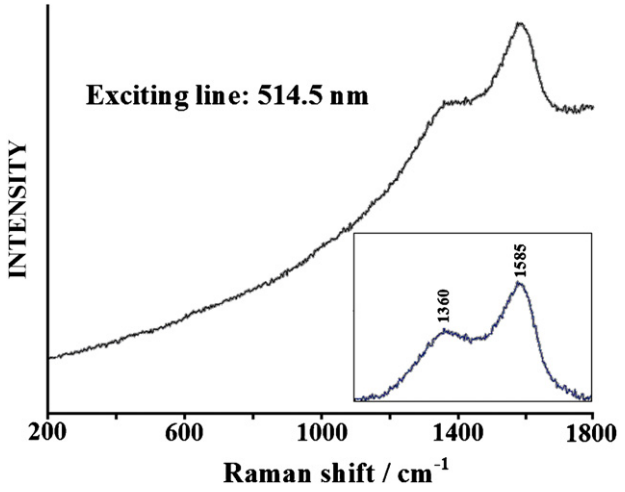

Fig. 6. Micro-Raman spectrum of Pd NPs in acetone, after drying on a solid substrate. In the inset the Raman spectrum is reported after background subtraction. Intensities in arbitrary units.

performed on Pd colloids produced at the same laser fluence but in an ultrapure water environment. As expected, in the XPS spectrum a sharp peak in the region characteristic of C 1s core transition and related to the atmospheric contamination is clearly detectable. This peak results however much weaker (less than the half) than the one found in case of acetone. Since the two samples were prepared and introduced in the analysis chamber following the same operation procedure, the larger amount of carbon observed on the acetone-prepared NPs cannot be due to environmental contamination alone but, more likely, it is in large part related to the nanoparticles. An indication of the presence of amorphous or graphitic carbon onto the NPs, rather than carbon present in form of acetone adsorbed on NPs surface, is provided by micro-Raman analysis of Pd NPs deposited on a polished and cleaned steel substrate, as visible in Fig. 6, showing the well known bands at about 1360 cm^{-1} (D band) and 1580 cm^{-1} (G band) of the amorphous carbon [29].

3.2. Alcohols: ethanol and 2-propanol

TEM images of NPs subsets in alcohols at both laser fluences show that they are spheroidal and well detached, as visible in Fig. 7 for ethanol and 2-propanol colloids obtained at a 21 J cm^{-2} laser fluence. No material is visible between and around nanoparticles ensembles. SAED pattern obtained from a subset of NPs in ethanol suggests that they are prevailingly crystalline (see Fig. 3b). The size distribution of particles in alcohols, as reported in Fig. 8 in the case of ethanol for 4 and 21 J cm^{-2} fluences, is narrow ($\sigma \sim 2$–3 nm) and peaked in the range 3–5 nm depending on experimental conditions.

As previously reported in several papers dealing PLAL [14,30], the increase of laser fluence results in a growth of nanoparticles dimensions (Fig. 8). When fluence is increased from 4 to 21 J cm^{-2}, the average size of nanoparticles in ethanol moves from 4.5 to 5.3 nm and in 2-propanol from 3.6 to 4.2 nm. In all the cases, the size distribution of NPs is mono-modal and the data are not satisfactorily fitted by using a single log-normal function, as reported in previous papers [12,31,32], due to an excess of large particles (see Fig. 8).

Similarly to what found in acetone and in water, XPS analysis of NPs obtained in alcohol shows the presence of palladium in different chemical environment. Accordingly to the Binding Energy values, both metallic ($3d_{5/2}$ peak at 335.2 ± 0.1 eV) and Pd^{2+} ($3d_{5/2}$ peak at 336.9 ± 0.1 eV) species are present at the sample surface (see Fig. 9). Here, however, the amount of oxidized palladium results lower with respect to the case of acetone-prepared NPs

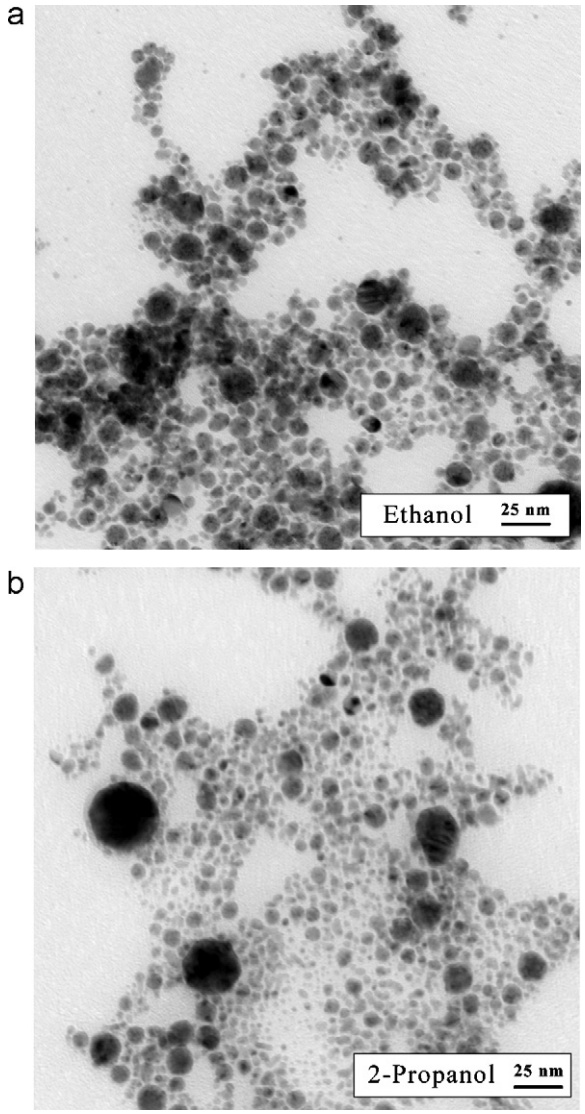

Fig. 7. TEM images of Pd NPs produced at 21 J cm^{-2} laser fluence in ethanol and 2-propanol solutions.

leading the ratio Pd^{2+}:Pd^0 to be approximately equal to 1:4, where such difference could be explained by the reducing properties of ethanol. Also in this case a strong carbon peak, which can be deconvolved into 3 contributions, is clearly detectable (see Fig. 9). The strongest of the three components (B.E. = 284.8 eV) was attributed to aliphatic or C^0 carbon, while the others (B.E. energy ~286 and 288 eV) were respectively assigned to carbon in alcohols/ethers and carboxyl groups. Also in this case the intensity of the carbon related peak is much higher with respect to the one recorded on water prepared NPs. It is therefore reasonable to suppose that it mainly derives from amorphous/graphitic carbon strictly related to the colloid and not due to environmental contamination alone, similarly to the case of acetone colloid.

3.3. Hydrocarbons: toluene and n-hexane

The production of NPs in n-hexane and toluene was attempted at different laser fluences but the process was inefficient and NPs were very unstable.

In n-hexane, at the end of the irradiation stage, the solution became opalescent but did not change noticeably colour, which agrees with the poor ablation rate measured by AAS. It was not

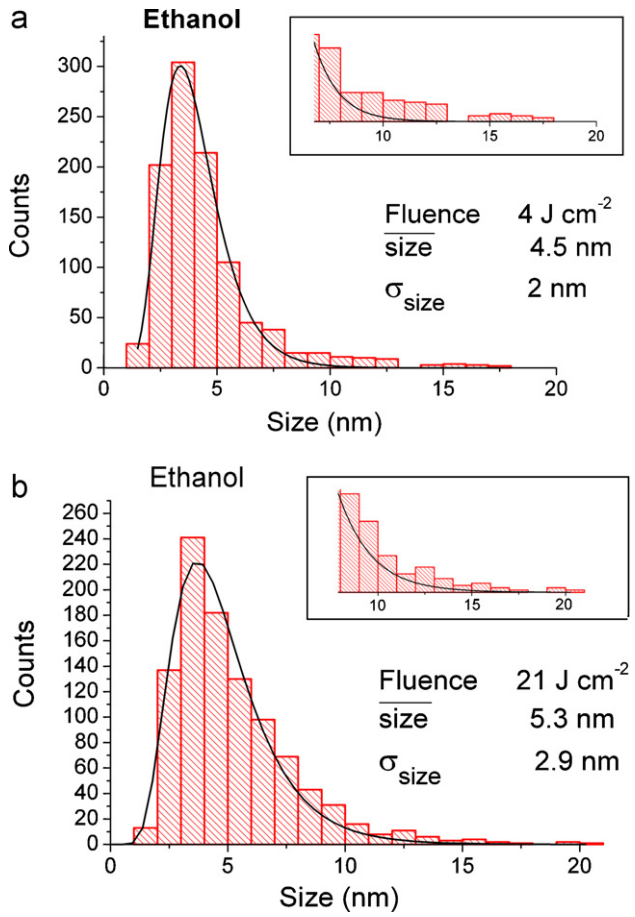

Fig. 8. Size distribution of nanoparticles produced in ethanol by using a laser fluence of 4 and 21 J cm^{-2}. The solid line represents the fit of the data by using a single log-normal function. In the inset a magnification of the region of larger size NPs is reported, showing the hard matching of size distributions with lognormal curve fitting.

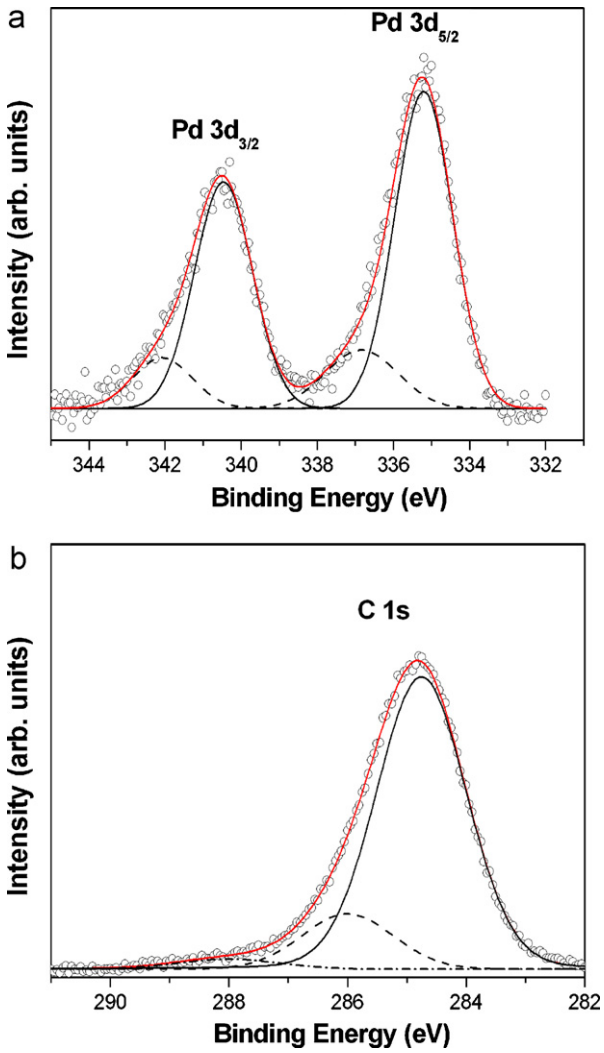

Fig. 9. XPS spectrum (circles represent row data) of NPs in ethanol. On the left is displayed the region of spectrum characteristic of the Pd 3d transitions; the solid curve refers to Pd^0 whereas the dashed curve refers to Pd^{2+}. On the right is displayed the region of spectrum characteristic of C 1s transition. The solid, dash and dash-dot curves refer to aliphatic, alcohols/ethers and carboxyls carbon respectively.

possible to increase the laser fluence without bursting the solvent due to the plasma formed at the solvent–air interface. The poor efficiency of ablation rate and NP formation was confirmed by the observation of UV–vis spectra, which show an extinction curve near the zero (Fig. 1). TEM images of n-hexane solution revealed the presence of a few nanoparticles surrounded by a gel-like material. The nanoparticles markedly deviate from a spherical shape showing evident signs of crystal facets.

Despite the lower ablation rate with respect to acetone and alcohols, the irradiation of the palladium target immersed in toluene initially appeared more efficient than in hexane, resulting in a colour change of the solution toward the yellow and then to the brown. However, most of the ablated material appears already deposited at the bottom of the vial after one day. Checking the extinction spectra of the colloids 1 month after the irradiation reveals a further reduction of NPs by a percentage going from 40% to 60% depending on the laser fluence, confirming a strong instability of nanoparticles.

TEM images of the toluene colloid (Fig. 10) evidence that most of the material is in a gel-like form, containing a few nanoparticles of irregular shape and signs of crystal facets. SAED patterns of such material shows a diffuse alone typical of amorphous material including a very few amount of crystalline structures (Fig. 3c). The micro-Raman analysis of the black material deposited at the bottom of the vial shows very strong bands from amorphous carbon, thus suggesting a strong presence of carbon in the nanoparticles and in the gel-like material where they are embedded.

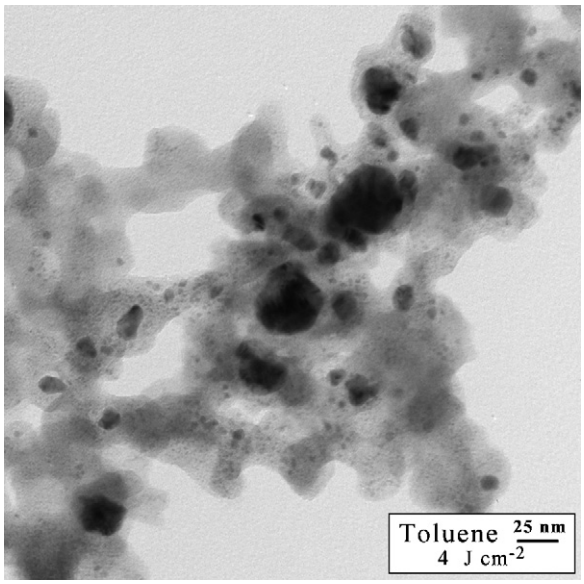

Fig. 10. TEM image of the colloid produced in toluene by a 4 J cm^{-2} laser fluence.

4. Discussion

The present investigation was motivated both by the general purpose of increasing the understanding of the solvent role in the process of NP formation and by the aim of exploring the possibility of producing colloids of Pd NPs in organic solvents by PLAL technique, to be used for specific catalytic applications. It is well known that, in case of ablation of metals in organic solvents, carbon can affect the final composition of the colloid in several ways, as it can be present in the form of pure NPs, as those produced in ordinary combustion processes [33] or by means of laser irradiation of organic solvents [34,35], can be incorporated in the metallic NPs, as reported by other authors [14,15], or again can constitute a carbon shell surrounding them [16,17].

In our results, the growth of NPs in an environment containing atoms originated by the solvent results in the presence of amorphous or graphitic carbon into NPs, as evidenced by XPS and Raman analyses on ethanol and acetone colloids and on the material deposited in the vial in toluene.

In the case of toluene, n-hexane but also in acetone at the largest laser fluence, a large amount of material, surrounding the NPs, is well visible in the colloid, similarly to what observed by Golightly and Castleman [14] after the irradiation of a Ti target in n-hexane, and by Amendola et al. [17], after the irradiation of an Au target in toluene. The inspection of HR-TEM images suggests that such material is not constituted by an ensemble of small NPs but it is rather a sort of gel-material, prevailingly amorphous, as evidenced by SAED patterns obtained in toluene colloids. According to Golightly and Castleman [14], such matter is probably constituted by a polymer carbon-rich matrix, produced by the pyrolysis of the solvent, enriched to a certain extent by Pd atoms. The presence of the carbon-matrix could have hindered the nucleation and growth of nanoparticles, as suggested by the small amount of NPs visible in TEM images in toluene (see Fig. 10) or by the lower UV–vis curve of acetone with respect to alcohols despite the similar ablation rate.

A similar result was found by Amendola et al. [17], irradiating an Au target in toluene. The small sizes of NPs observed was explained by the presence of a graphitic carbon matrix around them, resulting in the formation of an external graphitic shell and in the suppression of their characteristic Surface Plasmon Absorption band.

In case of toluene and n-hexane, the solvent seems also to have played a role in determining the formation of faceted crystal particles. The mechanism leading to a non-isotropic growth of particles cannot be easily explained by the mechanisms already discussed in literature, since in this case an anisotropy cannot be driven by local Surface Plasmon Resonances [36], by and external electric fields or by the presence of inorganic salts in the solution [37]. The understanding of the mechanism of preferential growth of NPs along some crystallographic planes requires dedicated investigations and is not further discussed here.

The dimensions of the NPs produced in organic solvents are slightly lower than those produced in water in the same conditions. As an example, at a fluence of 4 J cm^{-2}, the average size of NPs in water is 6.7 nm, while it lowers to 4.5 nm in ethanol, to 3.6 nm in 2-propanol and to 3.3 nm in acetone. Such result seems not to be related to the thermal properties of the solvents, which can affect the cooling times of the plume; in fact, the thermal conductivity of water is larger than that of the organic solvents and then it would result in a faster cooling of the plume and in smaller NPs. Also the different density of water (1 g/cm^3) with respect to that of organic solvents (~0.79 g/cm^3 for acetone, ethanol and 2-propanol), which can in principle affect the confinement/cooling rate of the plume and the collision rate inside the plume, appears too low to justify the different sizes observed. Therefore, the more plausible hypothesis is that NPs growth in organic solvents is hindered by the presence of carbon attached onto NPs surface, in graphitic or amorphous form, eventually constituting a protective shell, or alternatively by the carbon-rich matrix surrounding them [17].

The size distributions of NPs are hardly fitted by a single lognormal function because of an excess of large particles. Such feature was previously found for Pd NPs produced by PLAL in ultrapure water [12] as well as for other metallic NPs produced by PLAL [31,32]. The reason of testing such function relies on the fact that, in case of nucleation and successive growth of NPs via liquid-like coalescence, the logarithms of particles volumes should have a Gaussian distribution, so that particle size are lognormal distributed [38].

The reason of deviations from a lognormal function has been debated by many authors, who suggested that a real bimodal distribution could exist, produced by the concomitance of different mechanisms of particles formation, depending on different mechanisms of laser ablation (vaporization, melt splashing, spallation, phase explosion, plasma etching) [31,32], on different mechanisms of NP growth into the vapour [38], or finally on the occurrence of NPs fragmentation produced by the interaction with the laser beam [15,39]. Relying on the results reported in Ref. [12], we believe that in our case a real bimodal distribution of particles is not justified, and that the dimensions of nanoparticles are mainly dependant on their growth mechanism, rather than on the mechanisms of laser ablation or on photo-fragmentation process. According to the two step formation mechanism of NPs sketched by Mafune et al. [40], an early stage of embryonic particle formation in the hot plume is followed by a second stage in which they grow via liquid-like coalescence or via absorption of atomic vapour. It is possible that the deviations from a lognormal function can be produced by the relevance of atom-absorption mechanism in NP growth, which is competitive with the growth via liquid coalescence. In fact, according to Ref. [38], atomic absorption process is strongly affected by diffusion and then the size distribution becomes not adequately described by a log-normal function. Another possible cause of deviation from a log-normal function is the spatial inhomogeneity of the plume resulting in different cooling times of its different regions, leading to different dimensions of particles grown near the gas/liquid interface and in the core of the plume [41]. Finally, a non log-normal distribution could be expected for the non-stationarity of the ablation process, where at the beginning of the ablation stage the whole laser pulse energy reaches the target surface while, at later times, a considerable part of the pulse energy undergoes laser-NPs interaction and is absorbed in the secondary plasma at the solvent–air interface. In such scheme, the NPs produced at early times of ablation stage should be significantly larger than those produced at later times.

The stability of the colloidal suspensions generally depends on the presence of surface electric charges, due to strongly adsorbed species that impair aggregation between the dispersed particles. These charges induce a diffuse layer of opposite-sign electric charges in the dispersing medium around the particle. This two-layer charge structure is not present in liquids with low relative dielectric constant (ε_R), whereas it occurs in polar liquids like water ($\varepsilon_R = 81$) and, but to a lower extent, ethanol ($\varepsilon_R = 25$) or acetone ($\varepsilon_R = 21$). For example, we recently obtained stable Pd colloids in pure water by the presence of OH– or O– species on their surface, deriving from the aqueous environment [12]. In the literature, stable Pd colloids in organic solvents were obtained by adsorption on different polymers [42–46], which avoid the aggregation of the metal particles and, consequently, the coalescence of the colloidal suspensions. In the present case, the stability of the Pd colloids in pure acetone could be attributed to the formation of enolate anions (see Fig. 11a), which adsorb on the surface of the positively charged palladium particles, as obtained by laser ablation.

The existence of surface-bound acetone enolate was postulated on the basis of infrared spectroscopic measurements of acetone

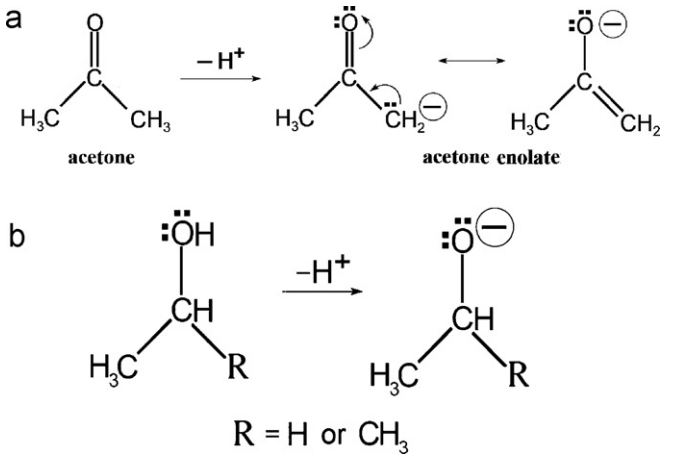

Fig. 11. Formation process of enolate (a) and alcoholate (b) anions in the acetone and alcohol colloids.

adsorbed on various metal oxides, on NiO [47], Fe_2O_3 [48] and Al_2O_3 [49,50]. Organometallic complexes of Ru [51] and Pd [52] containing acetone enolate are also known. On the other hand, the presence of acetone enolate was ascertained on Pt [53,54] and Ni [55], metals with the same electronic configuration of palladium. A similar effect was clearly observed in the production of AuNP in pure acetone [56].

Analogously, the stability of our Pd colloids obtained in alcohols could be related to adsorbed anions (alcoholates, see Fig. 11b) deriving from the dispersing medium. Otherwise, non polar solvents like toluene and n-hexane, unable to give rise to adsorbed anionic species, cannot provide any stabilization to the palladium nanoparticles, as experimentally found.

5. Conclusions

We have investigated the production of palladium nanoparticles via Pulsed Laser Ablation in Liquid by using several organic solvents, such as acetone, 2-propanol, ethanol, toluene and n-hexane. No surfactant agent was added to the solution for stabilizing the colloid. The morphology, composition, stability and oxidation state of the nanoparticles obtained were analyzed by TEM-EDS imaging, UV–vis spectroscopy, XPS spectroscopy and Raman spectroscopy, evidencing noticeable differences at varying the nature of the solvent utilized. Results suggest that the solvent strongly affects the laser ablation process, the growth process of the nanoparticles, thus determining their dimensions, and their stability. Significantly different ablation rates have been obtained in the different solvents; such spread, coupled to a negligible solvent absorption of the beam in all cases (except for water), suggests that the liquid should not be considered exclusively as a transparent/absorbing medium confining the plasma but rather as an environment playing an active role in laser ablation process (driven by its optical and thermodynamic properties), similarly to what happens in Laser-Supported Mechanisms in gas. It is also possible that the low ablation rate in toluene and n-hexane is driven by the presence of carbon-rich gel-like material, which affects the propagation of the laser beam toward the target surface and reduce the real impinging fluence.

In the case of acetone at low fluence ($4\,J\,cm^{-2}$) and alcohols NPs are spheroidal, non aggregated and stable. Comparing the results with those obtained in a previous paper, it emerges that they are slightly smaller than those produced in pure water (<size> = 6.7 nm), with average sizes in the 3–5 nm range. It is possible that smaller dimensions are related to the attachment onto the NPs surface of carbon atoms, as suggested by XPS and micro-Raman measurements, or of solvent molecules, that hinders the further growth of Pd nanoparticles. The hypothesis could be verified by TEM measurements of single nanoparticles at higher resolution, which would allow to verify the formation of an external carbon shell on particles, as observed in other works. The stability of the Pd colloids in pure acetone and in alcohols is attributed to the adsorption on the surface of the positively charged particles of enolate and alcoholates anions respectively, which hinder their aggregation because of electrostatic repulsion between particles.

In toluene and n-hexane a smaller amount of nanoparticles, surrounded by a carbon-rich gel-like material, is produced. The situation is similar to the case of acetone when the larger fluence is used ($21\,J\,cm^{-2}$). The material around the particles is mainly amorphous and is probably formed by the pyrolysis of the solvent. The poor efficiency of NPs formation is probably caused by the low ablation rate but also by the presence of the gel-like material that could have hindered their nucleation and growth. Particles formed in toluene and n-hexane are unstable decaying in a percentage of 40–60% during a month. This is attributed to the non polarity of the solvents, that hampers the formation of anions adsorbing on the NPs and stabilizing the colloid.

Acknowledgments

The authors gratefully thank the Italian Ministero dell'Università e Ricerca for the financial support. The work was supported by MIUR Grants PRIN 2008. F. Giammanco e and M. Muniz-Miranda wish to acknowledge funding from the project NABLA (Decree n.4508-September 1, 2010 by Regione Toscana-Italy, PAR FAS 2007-2013 funds, Action 1.1.a.3).

References

[1] S. Barcikowski, F. Mafuné, Trends and current topics in the field of laser ablation and nanoparticle generation in liquids, J. Phys. Chem. C 115 (2011) 4985.
[2] V. Amendola, M. Meneghetti, Controlled size manipulation of free gold nanoparticles by laser irradiation and their facile bioconjugation, J. Mater. Chem. 17 (2007) 4705–4710.
[3] V. Amendola, S. Polizzi, M. Meneghetti, Free silver nanoparticles synthesized by laser ablation in organic solvents and their easy functionalization, Langmuir 23 (2007) 6766–6770.
[4] F. Mafunè, J.Y. Kohno, Y. Takeda, T. Kondow, Formation of stable platinum nanoparticles by laser ablation in water, J. Phys. Chem. B 107 (2003) 4218–4223.
[5] D.K. Park, S.J. Lee, J.H. Lee, M.Y. Choi, S.W. Han, Effect of polymeric stabilizers on the catalytic activity of Pt nanoparticles synthesized by laser ablation, Chem. Phys. Lett. 484 (2010) 254–257.
[6] S. Kim, B.K. Yoo, K. Chun, W. Kang, J. Choo, M.S. Gong, S.W. Joo, Catalytic effect of laser ablated Ni nanoparticles in the oxidative addition reaction for a coupling reagent of benzylchloride and bromoacetonitrile, J. Mol. Catal. A: Chem. 226 (2005) 231–234.
[7] C.B. Hwang, Y.S. Fu, Y.L. Lu, S.W. Jang, P.T. Chou, C.R.C. Wang, S.J. Yu, Synthesis characterization and highly efficient catalytic reactivity of suspended palladium nanoparticles, J. Catal. 195 (2000) 336–341.
[8] S.Z. Mortazavi, P. Parvin, A. Reyhani, A.N. Golikand, S. Mirershadi, Effect of laser wavelength at IR (1064 nm) and UV (193 nm) on the structural formation of palladium nanoparticles in deionized water, J. Phys. Chem. C 115 (2011) 5049–5057.
[9] T. Nishi, A. Takeichi, H. Azuma, N. Suzuki, T. Hioki, T. Motohiro, Fabrication of palladium nanoparticles by Laser Ablation in Liquid, J. Laser Micro/Nanoeng. 5 (2010) 192–196.
[10] A. Biffins, M. Zecca, M. Basato, Palladium metal catalysts in heck C–C coupling reactions, J. Mol. Catal. A: Chem. 173 (2001) 249–274.
[11] J.M. Campelo, D. Luna, R. Luque, J.M. Marinas, A.A. Romero, Sustainable preparation of supported metal nanoparticles and their application in catalysis, ChemSusChem 2 (2009) 18–45.
[12] G. Cristoforetti, E. Pitzalis, R. Spiniello, R. Ishak, M. Muniz-Miranda, Production of palladium nanoparticles by pulsed laser ablation in water and their characterization, J. Phys. Chem. C 115 (2011) 5073–5083.
[13] A.M. Caporusso, P. Innocenti, L.A. Aronica, G. Vitulli, R. Gallina, A. Biffins, M. Zecca, B. Corain, Functional resins in palladium catalysis: promising materials for Heck reaction in aprotic polar solvents, J. Catal. 234 (2005) 1–13.
[14] J.S. Golightly, A.W. Castleman, Analysis of titanium nanoparticles created by laser irradiation under liquid environments, J. Phys. Chem. B 110 (2006) 19979–19984.
[15] A.V. Simakin, V.V. Voronov, N.A. Kirichenko, G.A. Shafeev, Nanoparticles produced by laser ablation of solids in liquid environment, Appl. Phys. A: Mater. Sci. Process. 79 (2004) 1127–1132.

[16] V. Amendola, P. Riello, M. Meneghetti, Magnetic nanoparticles of iron carbide, iron oxide, iron@iron oxide, and metal iron synthesized by laser ablation in organic solvents, J. Phys. Chem. C 115 (2011) 5140–5146.
[17] V. Amendola, G.A. Rizzi, S. Polizzi, M. Meneghetti, Synthesis of gold nanoparticles by laser ablation in toluene: quenching and recovery of the surface plasmon absorption, J. Phys. Chem. B 109 (2005) 23125–23128.
[18] S.I. Dolgaev, A.V. Simakin, V.V. Voronov, G.A. Shafeev, F. Bozon-Verduraz, Nanoparticles produced by laser ablation of solids in liquid environment, Appl. Surf. Sci. 186 (2002) 546–551.
[19] R.M. Tilaki, A. Iraji Zad, S.M. Mahdavi, Size, composition and optical properties of copper nanoparticles prepared by laser ablation in liquids, Appl. Phys. A 88 (2007) 415–419.
[20] F. Giammanco, E. Giorgetti, P. Marsili, A. Giusti, Experimental, Theoretical analysis of photofragmentation of Au nanoparticles by picosecond laser radiation, J. Phys. Chem. C 114 (2010) 3354–3363.
[21] K. Yamada, K. MiyaJima, F. Mafunè, Thermionic emission of electrons from gold nanoparticles by nanosecond pulse-laser excitation of interband, J. Phys. Chem. C 111 (2007) 11246–11251.
[22] J.A. Creighton, D.G. Eadon, Ultraviolet-visible absorption spectra of the colloidal metallic elements, J. Chem. Soc. Faraday Trans. 87 (1991) 3881–3891.
[23] W. Chen, W. Cai, Y. Lei, L. Zhang, A sonochemical approach to the confined synthesis of palladium nanoparticles in mesoporous silica, Mater. Lett. 50 (2001) 53–56.
[24] G. Cardenas-Trivino, R.A. Segura, J. Reyes-Gasga, Palladium nanoparticles from solvated atoms – stability and HRTEM characterization, Colloid Polym. Sci. 282 (2004) 1206–1212.
[25] U. Kreibig, M. Vollmer, Optical Properties of Metal Clusters, Springer-Verlag, Berlin, Heidelberg, 1995.
[26] V.A. Bondzie, P. Kleban, D.J. Dwyer, XPS identification of the chemical state of subsurface oxygen in the O/Pd(l10) system, Surf. Sci. 347 (1996) 319–328.
[27] M. Brun, A. Berthet, J.C. Bertolini, XPS, AES and auger parameter of Pd and PdO, J. Electron. Spectrosc. Relat. Phenom. 104 (1999) 55–60.
[28] E.H. Voogt, A.J.M. Mens, O.L.J. Gijzeman, J.W. Geus, Adsorption of oxygen and surface oxide formation on Pd(1 1 1) and Pd foil studied with ellipsometry, LEED, AES and XPS, Surf. Sci. 373 (1997) 210–220.
[29] M. Veres, M. Füle, S. Tóth, M. Koós, I. Pócsik, Surface enhanced Raman scattering (SERS) investigation of amorphous carbon, Diamond Relat. Mater. 13 (2004) 1412–1415.
[30] F. Mafune, J.Y. Kohno, Y. Takeda, T. Kondow, H. Sawabe, Formation size control of silver nanoparticles by laser ablation in aqueous solution, J. Phys. Chem. B 104 (2000) 9111–9117.
[31] W.T. Nichols, T. Sasaki, N. Koshizaki, Laser ablation of a platinum target in water. II. Ablation rate and nanoparticle size distributions, J. Appl. Phys. 100 (2006) 114912.
[32] A.V. Kabashin, M. Meunier, Synthesis of colloidal nanoparticles during femtosecond laser ablation of gold in water, J. Appl. Phys. 94 (2003) 7941–7943.
[33] G. Rusciano, A.C. De Luca, A. D'Alessio, P. Minutolo, G. Pesce, A. Sasso, Surface-enhanced Raman scattering study of nano-sized organic carbon particles produced in combustion processes, Carbon 46 (2008) 335–341.
[34] M.J. Wesolowski, S. Kuzmin, B. Moores, B. Wales, R. Karimi, A.A. Zaidi, Z. Leonenko, J.H. Sanderson, W.W. Duley, Polyyne synthesis and amorphous carbon nano-particle formation by femtosecond irradiation of benzene, Carbon 49 (2011) 625–630.
[35] A. Hu, J. Sanderson, Y. Zhou, W.W. Duley, Formation of diamond-like carbon by fs laser irradiation of organic liquids, Diamond Relat. Mater. 18 (2009) 999–1001.
[36] T. Tsuji, M. Tsuji, S. Hashimoto, Utilization of laser ablation in aqueous solution for observation of photoinduced shape conversion of silver nanoparticles in citrate solutions, J. Photochem. Photobiol. A 221 (2011) 224–231.
[37] P. Liu, H. Cui, C.X. Wang, G.W. Yang, From nanocrystal synthesis to functional nanostructure fabrication: laser ablation in liquid, Phys. Chem. Chem. Phys. 12 (2010) 3942–3952.
[38] C.G. Granqvist, R.A. Buhrman, Ultrafine metal particles, J. Appl. Phys. 47 (1976) 2200–2219.
[39] F. Bozon-Verduraz, R. Brayner, V.V. Voronov, N.A. Kirichenko, A.V. Simakin, G.A. Shafeev, Production of nanoparticles by laser-induced ablation of metals in liquids, Quant. Electron. 33 (2003) 714–720.
[40] F. Mafune, J.Y. Kohno, Y. Takeda, T. Kondow, H. Sawabe, Formation of gold nanoparticles by laser ablation in aqueous solution of surfactant, J. Phys. Chem. B 105 (2001) 5114–5120.
[41] S.B. Wen, X. Mao, R. Greif, R.E. Russo, Experimental and theoretical studies of particle generation after laser ablation of copper with a background gas at atmospheric pressure, J. Appl. Phys. 101 (2007) 123105.
[42] M. Harada, M. Ueji, Y. Kimura, Synthesis of colloidal particles of poly(2-vinylpyridine)-coated palladium and platinum in organic solutions under the high temperatures and high pressures, Colloids Surf. A 315 (2008) 304–310.
[43] S.H. Choi, Y.P. Zhang, A. Gopalan, K.P. Lee, H.D. Kang, Preparation of catalytically efficient precious metallic colloids by gamma-irradiation and characterization, Colloids Surf. A 256 (2005) 165–170.
[44] N. Jungmann, M. Schmidt, M. Maskos, Amphiphilic poly(organosiloxane) nanospheres as nanoreactors for the synthesis of topologically trapped gold, silver, and palladium colloids, Macromolecules 36 (2003) 3974–3979.
[45] N. Cioffi, L. Torsi, I. Losito, L. Sabbatini, P.G. Zambonin, T. Bleve-Zacheo, Nanostructured palladium-polypyrrole composites electrosynthesised from organic solvents, Electrochim. Acta 46 (2001) 4205–4211.
[46] S. Mecking, R. Thomann, H. Frey, A. Sunder, Preparation of catalytically active palladium nanoclusters in compartments of amphiphilic hyperbranched polyglycerols, Macromolecules 33 (2000) 3958–3960.
[47] H. Miyata, Y. Toda, Y. Kubokawa, Infrared studies of adsorption on MgO and NiO, J. Catal. 32 (1974) 155–158.
[48] G. Busca, V. Lorenzelli, Infrared study of the reactivity of acetone and hexachloroacetone adsorbed on haematite, J. Chem. Soc. Faraday Trans. I 78 (1982) 2911–2919.
[49] B.E. Hanson, L.F. Wieserman, G.W. Wagner, R.A.H. Kaufman, Identification of acetone enolate on (-alumina: implications for the oligomerization and polymerization of adsorbed acetone, Langmuir 3 (1987) 549–555.
[50] M.I. Zaki, M.A. Hasan, F.A. Al-Sagheer, L. Pasupulety, Surface chemistry of acetone on metal oxides: IR observation of acetone adsorption and consequent surface reactions on silica-alumina versus silica and alumina, Langmuir 16 (2000) 430–436.
[51] F. Hartwig, R.G. Bergman, R.A. Anderson, Oxygen- and carbon-bound ruthenium enolates: migratory insertion, reductive elimination, beta.-hydrogen elimination, and cyclometalation reactions, Organometallics 10 (1991) 3326–3344.
[52] J. Vicente, J.A. Abad, M.T. Chicote, M.D. Abrisqueta, J.A. Lorca, M.C.R. de Arellano, Synthesis of new ketonyl palladium(II) and platinum(II) complexes with nitrogen-donor ligands. Crystal structure of [Pt{CH2C(O)Me}2(bpy)], Organometallics 17 (1998) 1564–1568.
[53] M.A. Vannice, W. Erley, H. Ibach, A RAIRS and HREELS study of acetone on Pt(1 1 1), Surf. Sci. 254 (1991) 1–11.
[54] E.L. Jeffery, R.K. Mann, G.J. Hutchings, S.H. Taylor, D.J. Willock, A density functional theory study of the adsorption of acetone to the (1 1 1) surface of Pt: implications for hydrogenation catalysis, Catal. Today 105 (2005) 85–92.
[55] W.S. Sim, T.C. Li, P.X. Yang, B.S. Yeo, Isolation and identification of surface-bound acetone enolate on Ni(1 1 1), J. Am. Chem. Soc. 124 (2002) 4970–4971.
[56] E. Giorgetti, M. Muniz-Miranda, P. Marsili, F. Giammanco, Stable gold nanoparticles obtained in pure acetone by laser ablation with different wavelengths, J. Nanopart. Res., in press.